PHYSICAL REVIEW B **74**, 161301(R) (2006)

Spin selective spectroscopy of a quantum dot using tunnel-coupled quantum wires as spin filters

K. Hitachi,[1] M. Yamamoto,[2,3] and S. Tarucha[2,4]
[1]*Department of Physics, The University of Tokyo, Hongo, Bunkyo-ku, Tokyo, 113-0033, Japan*
[2]*Department of Applied Physics, The University of Tokyo, Hongo, Bunkyo-ku, Tokyo, 113-8656, Japan*
[3]*SORST-JST, Kawaguchi-shi, Saitama, 331-0012, Japan*
[4]*ICORP Quantum Spin Project, Japan Science and Technology Agency, Hongo, Bunkyo-ku, Tokyo, 113-8656, Japan*
(Received 8 May 2006; revised manuscript received 5 September 2006; published 11 October 2006)

A quantum dot (QD) having two tunnel-coupled quantum wires (QWs) was fabricated to probe the QD's spin configuration using the QWs as spin filters. The QWs were adjusted to be either spin-polarized or spin-depolarized under a magnetic field B. The spin filtering effect was only observed for spin-polarized QWs, and singlet and triplet states were distinguished for values of the filling factor $2<\nu<4$. The spin filtering rate increased due to Zeeman splitting in the QW as the B field was increased, but it decreased dramatically the region of $\nu<2$ due to the cotunneling effect.

DOI: 10.1103/PhysRevB.74.161301 PACS number(s): 73.63.Kv, 73.63.Nm, 72.25.Dc

The ability to generate, manipulate, and probe electron spin is indispensable for the potential application of nanoscale devices to spintronics and quantum computation, and has recently been achieved using semiconductor quantum dots (QDs).[1–3] This is due to the intrinsic nature of electron spin, namely that the spin degree of freedom is well isolated from the environment. The spin-flip relaxation time T_1 is consequently much longer than the corresponding time for the orbital degrees of freedom.[3,4] T_1 can be even longer for QDs because of their reduced spin-scattering mechanisms such as the phonon-assisted spin-orbit interaction[5] and the hyperfine interaction.[6,7] As a consequence, spin relaxation hardly occurs during the electron transport through the QD. This makes it possible to perform spin-selective spectroscopy with a QD, using contact leads as spin filters.

The electron spin in a QD is strongly related to its orbital state and electronic correlation.[8,9] For example, a QD having an even number of electrons in the ground state can be in either a spin-singlet or a spin-triplet state depending on the applied magnetic field.[10] Singlet-triplet transitions were previously studied for a QD having a filling factor in the vicinity of two using magnetic edge states in a two-dimensional electron gas (2DEG) as contact leads.[1] The spin filtering is caused by the difference in the distance from the edge state to the QD or the tunneling probability between spin-up and spin-down electrons.

In this Rapid Communication, we report on spin selective spectroscopy for a QD using two quantum wires (QWs) as spin filters. This approach is similar to that of Ref. 1, but the spin filtering is caused by the spin polarization of the QWs, which is tunable with gate voltage, rather than by magnetic edge states. This allows us to study the QD spin configuration over a wide filling factor range and also to quantify the spin filtering effect depending on the Zeeman splitting or degree of spin polarization in the QWs. We set the QWs to be either spin-depolarized or spin-polarized and measured the single electron tunneling current. We only observed the spin filtering effect using the spin-polarized QWs, and we could distinguish the spin configurations in the QD in the filling factor range between two and four.

Our device consists of a QD with two tunnel-coupled QWs, i.e., left and right quantum wires, QWL and QWR, made in a 2DEG of an n-AlGaAs/GaAs heterostructure using the split-gate technique [see Fig. 1(a)]. The 2DEG has a sheet carrier density of 3.8×10^{15} m^{-2} and a mobility of 180 m^2/(Vs) at 1.5 K. The voltages V_{gP}, and V_{gTL} (V_{gTR}) are used to adjust the electrostatic potential of the QD, and the coupling between the QWL (QWR) and the QD, respectively. The voltage V_{gL} (V_{gR}) is used to adjust the width of the QWL (QWR). When a magnetic field B is applied perpendicular to the 2DEG plane, a spin-resolved plateau appears in the conductance G of QWL (R) at $G=e^2/h$. We adjust the gate voltages V_{gL} and V_{gR} to tune the QW conductance of $G=ne^2/h$ with $n=1$or 2, such that either a spin-polarized ($n=1$) or a spin-depolarized ($n=2$) state is formed in the QWs. We measure the single electron tunneling current through the QWL-QD-QWR structure as a function of V_{gP} and B. We use a standard low frequency lock-in technique with an excitation voltage of 5 μV to measure the conductance of the device. The electron temperature is 180 mK.

Figure 1(b) shows the QWR conductance vs V_{gR} measured for various B fields. Each circle represents the left edge of the first and second spin-depolarized plateaus with $G=2e^2/h$ and $4e^2/h$. Even for $B=0$ T, these plateaus are well resolved. As the B field is increased, these circles shift to less negative gate voltages and the plateaus become wider, reflecting an increase in the effective confinement energy. Spin-polarized plateaus also appear at $G=e^2/h$ and $3e^2/h$ for $B>1$ T. The left edges of these plateaus are indicated by open squares. We also measured the QWL conductance in the same way. Similar conductance plateaus are observed for $B>1$ T. The first spin-polarized plateau appears almost at the same V_{gR} (V_{gL} for QWL) for 1.5 T $<B<$ 2.4 T. We thus use such V_{gR} (V_{gL}) labeled A1 (B1) where $G=e^2/h$ at $B=2$ T to prepare the spin-polarized leads, and similarly V_{gR} (V_{gL}) labeled A2 (B2) where $G=2e^2/h$ at $B=2$ T to prepare the spin-depolarized leads. Note we only need one spin-polarized QW to apply the spin filtering effect.

Figure 2(a) shows a color scale plot of the Coulomb peaks evolving with B field observed with the spin-depolarized QW leads. The Coulomb peaks form zigzag structures, which shift up and down alternatively as the B field is in-

 ©2006 The American Physical Society

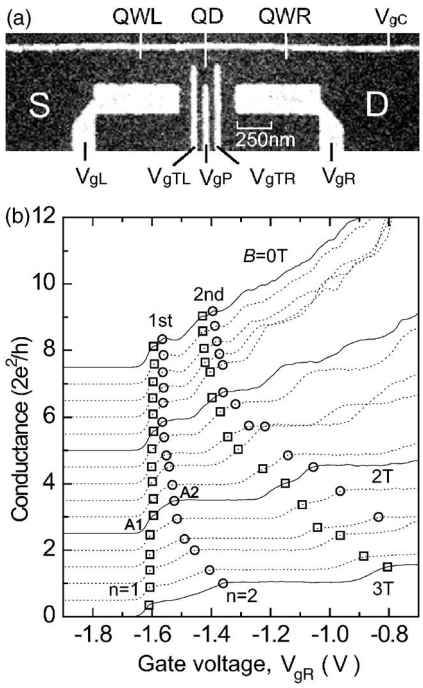

FIG. 1. (a) SEM photo of the device. A QD and two QWs, QWL and QWR, are defined by the white Schottky gates. (b) Conductance of the QWR as a function of V_{gR} and B. The B field is varied from 0 to 3 T with a 0.2 T step. For clarity, each curve is offset by $0.5\times e^2/h$ to the bottom. Symbols and labels A1 and A2 are explained in the text.

creased. Those shifted down (up) correspond to the filling of the lowest (second lowest) Landau states LL0 (LL1). The LL1 peaks are observed for small values of B and are labeled with triangles. Those labeled with solid triangles are not so well resolved, but are easier to identify in the measurement using the spin-polarized QW [see Fig. 2(b)]. The LL0 peaks are larger than the LL1 peaks because of the orbital effect. The electron wave function of the LL0 states spreads out in the QD, while that of the LL1 states is more localized in the center, so that the LL0 states are more strongly tunnel-coupled to the leads.[11] However, for the LL0 peaks we see no clear intensity modulation associated with possible transitions in the spin states. This implies that the magnetic edge states are not well resolved in the leads as to give rise to the spin filtering effect. In the following paragraphs we concentrate on the LL0 peaks to investigate the spin filtering effect independent of the orbital effect.

Figure 2(b) is the same plot as Fig. 2(a) but was measured with $n_R=1$ for the QWR and $n_L=2$ for the QWL. The Coulomb peaks evolve with the B field in a similar manner as those in Fig. 2(a). However, for all LL0 peaks we observe alternating intensity changes to the left and right of each triangle. We performed a more detailed measurement using the same method as the previous measurement but using spin polarized QWs for both leads. The result is shown in Fig. 3(a). The solid lines are guides indicating the peak shifts and intensity changes with the B field. The thick, medium, and thin lines represent the large, medium, and small peaks, respectively. It is evident that each LL0 peak alternates between small and large with the B field bounded by each

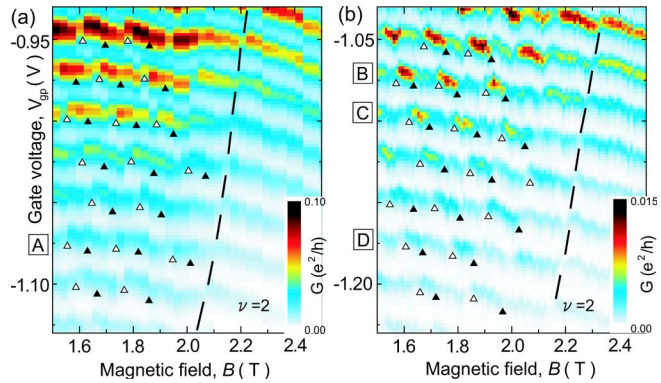

FIG. 2. (Color online) Intensity plot of Coulomb peaks evolving with B field measured with (a) $n_L=2$ QWL and $n_R=2$ QWR and (b) $n_R=1$ QWR and $n_L=2$ QWL. The QD enters the regime of filling factor $\nu=2$ to the right of the dashed line. The peak shifting down (up) compares to the filling of the lowest (second lowest) Landau states LL0 (LL1). The LL1 peaks are labeled with open and solid triangles.

triangle, indicating repeated transitions in the spin configuration. These features can also be seen in Fig. 2(b) on close examination of the data.

To account for the spin-dependent conductance observed in Figs. 2(b) and 3(a), we first consider a simple model with one ($N=1$) or two ($N=2$) electrons trapped by two single particle orbital states. The one electron state is always a spin doublet state having a total spin of $S=1/2$. When $N=2$, if the two orbital states are energetically well separated by an amount $\Delta\epsilon$ that is larger than the exchange energy K (<0), the ground state (GS) will be a spin singlet state with $S=0$ having two antiparallel spin electrons in the lower-lying orbital state. On the other hand, if the two orbital states are sufficiently close to each other that the condition $\Delta\epsilon<|K|$ is satisfied, the GS will be a triplet state with $S=1$ having one electron in each orbital state. In general, in the region of $2<\nu<4$, the GS is either a spin singlet or a triplet state for even N and always a spin doublet state for odd N.[12] In this region, the LL0 (LL1) states shift to low (high) energy with increasing B field, so that a triplet state appears whenever a LL0 state and a LL1 state intersect each other. We apply this argument to draw a state diagram in the B field and energy plane shown in Fig. 3(b). The number of electrons increases by one when crossing the zigzag solid line from above, which corresponds to the peak evolution with the B field in Fig. 3(a). Thick, medium, and thin solid lines are equivalent to those in Fig. 3(a). A unique electronic configuration is established in each honeycomb bounded by the solid and dotted lines. When the QWs are spin-polarized, i.e., $N_\uparrow>N_\downarrow$, where $N_{\uparrow(\downarrow)}$ is the number of spin-up (spin-down) electrons in the QW leads, Coulomb peaks associated with tunneling of spin-up electrons are larger than those associated with spin-down electrons. Therefore, the Coulomb peaks should be large when adding a spin-up electron to the $N-1$ doublet state to form the N-electron triplet state, and to the N-electron singlet state to form the $(N+1)$-electron doublet state. Note that the diagram of Fig. 3(b) is consistent with calculations based on the full 3D spin density functional theory.[12]

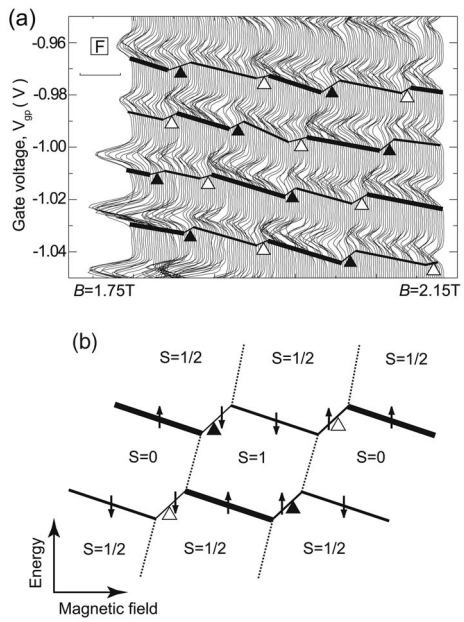

FIG. 3. (a) Evolution of Coulomb peaks with B field measured using the $n_R=n_L=1$ QWs. For clarity, each curve is horizontally offset. The bar in the figure is a conductance scale of $0.025e^2/h$. The zigzag solid line is a guide that indicates the changes in the peak position and intensity. The triangles correspond to those in Figs. 2(a) and 2(b). (b) State diagram to account for the experimental data of Figs. 2(b) and 3(a). The lines and symbols are the same as those in (a). Arrows indicate up or down spins to be added to form the states just above.

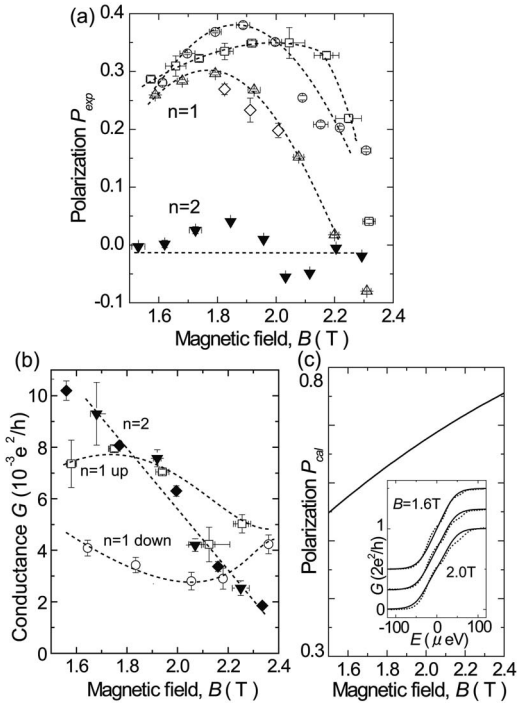

FIG. 4. (a) B field dependence of spin polarization P_{exp} derived from the data of peak A (▼) in Fig. 2(a), peaks B (□), C (○), and D (△) in Fig. 2(b) and peak F(◇) in Fig. 3(a). Strong B field dependence of P_{exp} is only detected using the spin-polarized $n=1$ QW(s). (b) B field dependence of Coulomb peak intensity $G_\uparrow(G_\downarrow)$ for adding a spin-up (spin-down) electron to the LL0 states. Symbols indicate $n=2$ $G_\uparrow$ (▼) and $n=2$ $G_\downarrow$ (◆) for peak A and $n=1$ $G_\uparrow$ (□) and $n=1$ $G_\downarrow$ (○) for peak D. (c) B field dependence of spin polarization P_{cal} calculated assuming a Zeeman splitting and thermal populations of spin-up and spin-down electrons (180 mK) in the QW. Inset: Calculation (solid lines) and experimental data (dotted lines) of the QWR conductance at $B=1.6, 1.8$, and 2.0 T, respectively.

Here we analyze the observed tunneling conductance to quantify the spin filtering effect of the spin-polarized QW lead. Figure 4(a) shows the conductance polarization rate defined as $P_{exp}=(G_\uparrow-G_\downarrow)/(G_\uparrow+G_\downarrow)$, where $G_\uparrow$ $(G_\downarrow)$ is the spin-up (spin-down) conductance of the down-shifting LL0 peaks labeled A in Fig. 2(a) and those labeled B–D in Fig. 2(b). $G_\uparrow(G_\downarrow)$ is derived by first averaging over the B field range for which the same type of LL0 peaks are observed and then interpolating between $G_\uparrow$ and $G_\downarrow$ to compare the spin-up and spin-down conductance in the same B field range. It is evident that $P_{exp}\approx 0$ for peak A, whereas for peaks B–D, P_{exp} gradually increases with increasing B up to 1.9 T, and then dramatically decreases near the $\nu=2$ region. This abrupt reduction in P_{exp} starts at a lower B field for peak C than for peak B and at a lower B field for peak D than for peak C, i.e., when each peak approaches the $\nu=2$ region. Note that the Coulomb peak in the more negative gate voltage approaches the $\nu=2$ region in the lower B field (see Fig. 2). These features are generally observed for the other Coulomb peaks as well. P_{exp} obtained for peak F in Fig. 3(a) is also shown in Fig. 4(a), and the B field dependence is similar to that of peak D. By contrast, no spin filtering was observed for peak A. That is, the spin polarization is only detected using the spin-polarized $n=1$ QW(s). This is different from the result of Ref. 1, probably because in our device the effective QW width at A2 in Fig. 1(b) is too small to form well-resolved edge states. Therefore, we assume that the large polarization observed for peaks B–D and F is only due to the spin-polarization of the QW. The increase in P_{exp} with increasing B field for $\nu>2$ is attributed to the increased Zeeman splitting in the QW. The abrupt decrease in P_{exp} observed for $\nu<2$ is probably due to cotunneling through the excited states (ESs) in the QD because spin-up electrons can tunnel through ESs even when spin-down electrons are only able to tunnel through the GS. Such ESs approach the GS as the B field increases, and become almost degenerate with the GS near $\nu=1$.

The discussion here about P_{exp} is well supported by the B dependencies of $G_\uparrow$ and $G_\downarrow$ shown in Fig. 4(b). For peak A, both $G_\uparrow$ and $G_\downarrow$ rapidly decrease with increasing B field above $B=1.5$ T. A similar but somewhat weaker B field dependence is observed for peak D for $B>2.3$ T or near the $\nu=2$ region, in which $G_\downarrow$ increases to the level of $G_\uparrow$. These features are also observed for the other Coulomb peaks including peak F. The conductance reduction with B field is assigned to magnetic squeezing of the electron wave function in the QD as well as in the QW leads. The weak B field dependence of peak D is probably because the ability of the B field to squeeze the electron wave function is weaker in the QWR with $n_R=1$ than with $n_R=2$. The increase of $G_\downarrow$ in the

$\nu=2$ region for peak D is due to tunneling through the ESs as described above.

We finally discuss the effect of Zeeman splitting in the QW leads on the conductance. Since the density of k states $D(k)$ is constant in one dimension we only consider the Fermi distribution function,

$$f_{\uparrow(\downarrow)} = \frac{1}{e^{\beta(E-(+)(1/2)|g^*|\mu B)} + 1}$$

to derive the spin-up (spin-down) electron population, $f_\uparrow(f_\downarrow)$, and calculate the spin polarization given by $P_{cal}=(f_\uparrow - f_\downarrow)/(f_\uparrow + f_\downarrow)$, where $|g^*|\mu B$ ($g^*=-0.44$) is the Zeeman splitting energy and E is the measurement energy. Here we assume the potential confinement to be constant with the B field. We also assume that the QW conductance is proportional to $f_\uparrow + f_\downarrow$. The inset of Fig. 4(c) shows the conductance calculated for three different B fields. The dotted lines are the experimental data taken from Fig. 2(a), which are laterally scaled to fit the calculated data by assuming that the increment of the gate voltage is proportional to that of energy. In this calculation the gate voltage V_{gR} used for the QWR with $n_R=1$ is set to the energy $E=0$ μeV. The observed QW conductance is well reproduced assuming the g factor $g^*=-0.44$. Figure 4(c) shows the calculated B field dependence of P_{cal} at $E=0$. The value of P_{cal} increases as the B field is increased, reflecting the increase in the Zeeman splitting. This behavior is qualitatively consistent with that of P_{exp} for $\nu>2$. However, for the quantitative comparison, we need a more rigorous treatment including the cotunneling effect.[13] This effect will be more important as the B field approaches the regime of $\nu=1$, as described before. Here we neglect spin relaxation due to spin-orbit coupling,[5] because the tunneling time is of the order of ns, which is much shorter than the spin relaxation time.[3,4]

In conclusion, we investigated single electron transport though a QD using tunnel-coupled QWs as spin filters. By tuning the spin polarization of the QW leads, we observed spin-filtered current through the QD and identified the spin configurations in the QD for $2<\nu<4$. We found that the observed spin filtering effect increases by the Zeeman effect in the QW with increasing B field for $\nu>2$, but it decreases for $\nu<2$ due to the cotunneling effect.

We acknowledge financial support from the Grant-in-Aid for Science Research A (No. 40302799), the Special Coordination Funds for Promoting Science and Technology, CREST-JST, and the QuIST program (DAAD 19-01-1-0659). We also thank Y. Tokura for helpful discussions.

[1] M. Ciorga, A. S. Sachrajda, P. Hawrylak, C. Gould, P. Zawadzki, S. Jullian, Y. Feng, and Z. Wasilewski, Phys. Rev. B **61**, R16315 (2000).

[2] J. A. Folk, R. M. Potok, C. M. Marcus, and V. Umansky, Science **299**, 679 (2003).

[3] J. M. Elzerman, R. Hanson, L. H. Willems van Beveren, B. Witkamp, L. M. K. Vandersypen, and L. P. Kouwenhoven, Nature (London) **430**, 431 (2004).

[4] T. Fujisawa, D. G. Austing, Y. Tokura, Y. Hirayama, and S. Tarucha, Nature (London) **419**, 278 (2002).

[5] A. V. Khaetskii and Y. V. Nazarov, Phys. Rev. B **61**, 12639 (2000).

[6] S. I. Erlingsson, Y. V. Nazarov, and V. I. Fal'ko, Phys. Rev. B **64**, 195306 (2001).

[7] K. Ono and S. Tarucha, Phys. Rev. Lett. **92**, 256803 (2004).

[8] L. P. Kouwenhoven, D. G. Austing, and S. Tarucha, Rep. Prog. Phys. **64**, 701 (2001).

[9] S. Tarucha, D. G. Austing, T. Honda, R J. van der Hage, and L. P. Kouwenhoven, Phys. Rev. Lett. **77**, 3613 (1996).

[10] S. Tarucha, D. G. Austing, Y. Tokura, W. G. van der Wiel, and L. P. Kouwenhoven, Phys. Rev. Lett. **84**, 2485 (2000).

[11] P. L. McEuen, E. B. Foxman, Jari Kinaret, U. Meirav, M. A. Kastner, N. S. Wingreen, and S. J. Wind, Phys. Rev. B **45**, 11419 (1992).

[12] M. Stopa, W. G. van der Wiel, S. De Franceschi, S. Tarucha, and L. P. Kouwenhoven, Phys. Rev. Lett. **91**, 046601 (2003).

[13] Patrik Recher, E. V. Sukhorukov, and Daniel Loss, Phys. Rev. Lett. **85**, 1962 (2000).